

On the Liquid–Liquid Phase Transition in Dense Hydrogen

V. V. Karasiev,¹ J. Hinz,¹ S. X. Hu,¹ and S. B. Trickey²

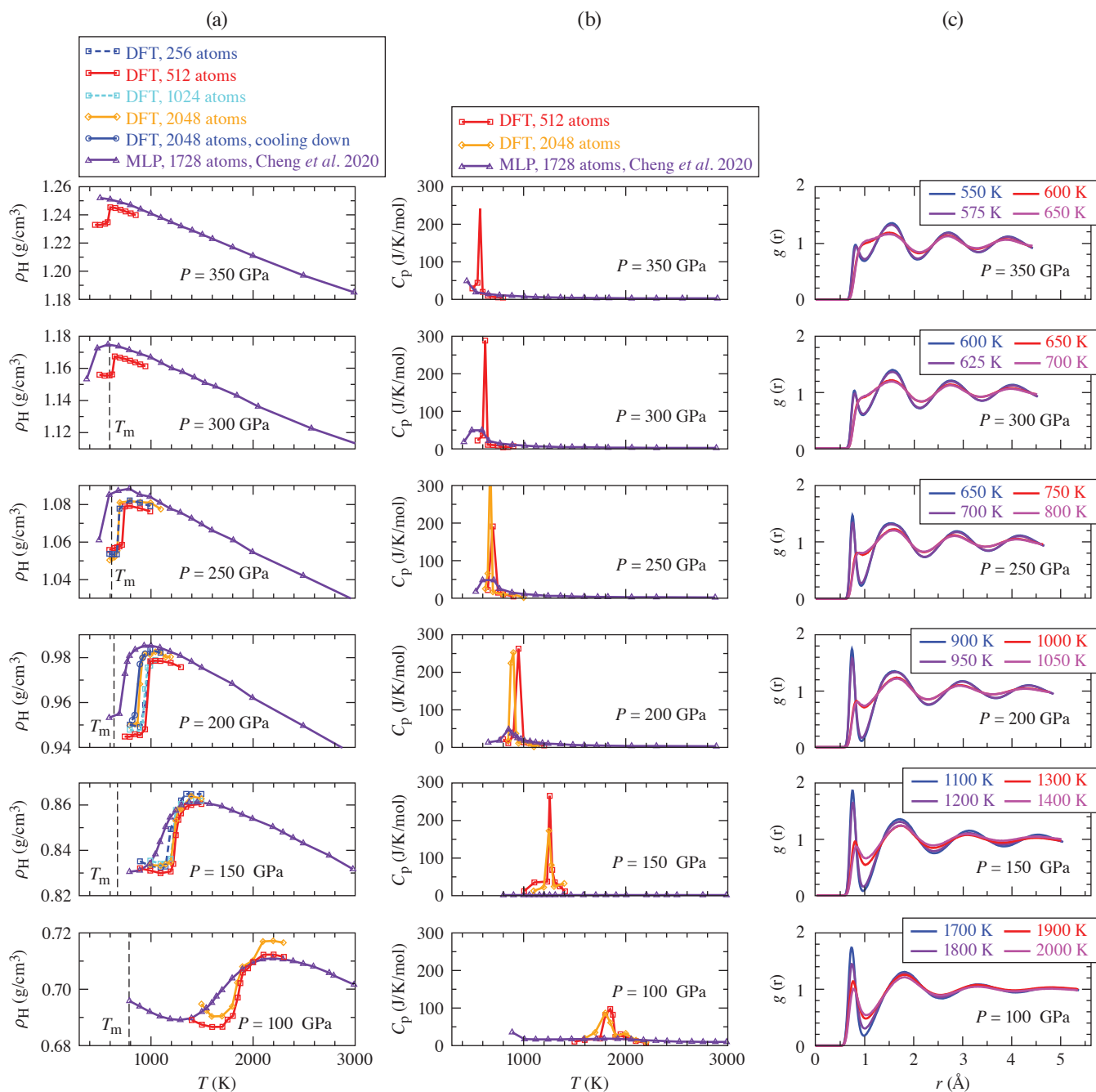
¹Laboratory for Laser Energetics

²Quantum Theory Project, Department of Physics, University of Florida

Determining the liquid–liquid phase transition (LLPT) in high-pressure hydrogen is a longstanding challenge with notable variation in experimental and calculated results (see Refs. 1–5 and citations therein). Until recently, the computational consensus was for a first-order transition. Calculated values differed but, for example, our results on $700 \leq T \leq 3000$ K are a curve along $320 \geq P \geq 70$ GPa (Ref. 2). Driven by molecular H₂ dissociation, transition signatures include density jumps, qualitative and sharp changes in ionic pair correlation functions (PCF's), and abrupt dc conductivity and reflectivity changes. In distinct contrast, Cheng *et al.*⁶ used molecular dynamics (MD) driven by a machine-learned potential (MLP) and found a continuous molecular-to-atomic liquid transformation that goes supercritical above $P \approx 350$ GPa, $T \approx 400$ K. They attributed the qualitative difference from MD-DFT (density functional theory) to (a) finite size effects that foster the formation of defective solids, with the common use of *NVT* dynamics tending to increase defect concentration relative to *NPT* ensemble results and (b) much shorter simulation times in the MD-DFT calculations than in the MD-MLP ones. Conceptually, the issue is whether a single MLP can correctly represent two chemically distinct regimes (molecular, atomic). An unambiguous test is to perform longer MD-DFT runs on significantly larger systems. If the MD-MLP represents the underlying theory (*ab initio* MD) faithfully and if the diagnosis based on MD-MLP is correct, results from the two simulation types should match. To test that, we have done much larger, longer MD-DFT calculations. The results are consistent with earlier MD-DFT calculations, thus qualitatively different from the MD-MLP results. Neither the large-system nor longer-run diagnosis from MD-MLP is sustained. Our *NPT* MD simulations were driven by DFT forces with Perdew–Burke–Ernzerhof (PBE) exchange correlation (XC).⁷ (Reference 6 used PBE to train the MLP.) We used from 256 through 2048 atoms per cell. Brillouin zone sampling used the Baldereschi mean value point for the simple cubic crystal structure $\mathbf{k} = (1/4, 1/4, 1/4)$ (Ref. 8). *VASP*^{9,10} was used for 1024 and 2048 atom systems, while the *i-PI* interface¹¹ with *Quantum Espresso*¹² was used for 256 and 512 atoms. Consistent results from the two confirm that the MD code and technical choices (thermostat, barostat, etc.) are inconsequential.

Our new large-system MD-DFT results agree with prior MD-DFT and coupled electron–ion Monte Carlo simulations:^{2,3,13} there is a sharp molecular-to-atomic transition. Figure 1 shows the qualitatively different character versus the MD-MLP prediction. Figure 1(a) shows density profiles $\rho_{\text{H}}(T)$ along isobars. At 300 and 350 GPa, the large-scale MD-DFT $\rho_{\text{H}}(T)$ values jump $\approx 1\%$ near $T = 650$ K. At 300 GPa, that is above the experimental melting temperature T_{m} (Ref. 14). In contrast, the 300-GPa MD-MLP isobar has a steep density increase near $T = 500$ K (in the stable solid phase),⁶ but it passes smoothly through both the melt line and the LLPT. Except for a systematic offset, the MD-MLP $\rho_{\text{H}}(T)$ matches the MD-DFT $\rho_{\text{H}}(T)$ in the atomic fluid region.

The molar heat capacity from MD-DFT as a function of T is shown in Fig. 1(b). All the isobars exhibit divergent heat capacity character across the transition. Evidently finite-size effects on T_{LLPT} are small and do not modify that character. To check on the possibility that finite-size effects trapped our simulations in defective solid configurations, we calculated the mean-squared displacement (MSD) of the 512 atom systems as a function of time along the 150- and 200-GPa isobars for $1100 \leq T \leq 1400$ K and $900 \leq T \leq 1200$ K, respectively. The MSD (not shown here) grows near linearly with time, as is characteristic of a liquid but not a solid.



TC15635JR

Figure 1

Comparison of MD results from the PBE XC-based MLP and *ab initio* MD-DFT (DFT) *NPT* simulations. (a) Hydrogen density as a function of T along six isobars. Experimental melting temperature T_m for each isobar is shown by a vertical dashed line.¹⁴ (b) Molar heat capacity as a function of T along the isobars. (c) PCF for each isobar for two temperatures below the density jump and two temperatures above the density jump.

Figure 1(c) shows the PCF on each isobar at temperature pairs below and above the density jump. Above, the first PCF peak virtually disappears, confirmation of the density jump being in conjunction with the molecular dissociation.²

To test possible long simulation duration effects on T_{LLPT} or its character, we performed six sequential MD-DFT runs of roughly 1.8-ps duration each for a total of ≈ 10 -ps duration and at 200 GPa with 512 and 2048 atoms. There were no meaningful differences in the results in either case. This outcome agrees with that of Geng *et al.*¹⁵ who performed runs up to 6 ps and found no meaningful differences with respect to 1.5 ps (after equilibration). To investigate whether the nanosecond time scale might make the simulated transition smooth, we performed a set of 2048-atom MD-DFT *NPT* simulations beginning with the atomic fluid at 200 GPa. Starting at 950 K, we cooled the system in sequential runs to 899, 849, and 824 K with simulation duration around 8 ps for each temperature. If the nanosecond time scale were to yield a smooth transition, the hydrogen density during such a fast cooling curve would not drop sharply below the hypothetical smooth long-duration curve. But, as evident in the Fig. 1(a) density plot at 200 GPa, the cooling curve (thin blue curve, circles) is almost identical to the one from MD-DFT simulations when the molecular fluid T is increased gradually (sharp transition shown by the solid orange curve).

Figure 2 shows the LLPT curves associated with density jumps, heat capacity peaks, and PCF peak disappearance. For the new large-scale MD-DFT calculations, those three criteria give one curve shown in red with squares at data points. With virtually identical P, T values; small differences in the transition temperature (less than 100 K for $P \leq 150$ GPa) are caused by numerical errors in calculating the molar heat capacity using finite differences. Two MD-MLP curves emerge from the analysis, however, one for the location of molar heat capacity maxima, C_P^{max} , and another for the maximum density, ρ_P^{max} . Consistent with the foregoing discussion, there are striking differences. The MLP C_P^{max} curve lies well below the MD-DFT curve. The MLP ρ_P^{max} curve is flatter than the MD-DFT reference curve and lies close to it only at about $P = 70$ GPa, $T = 2800$ K and then again for P between about 170 and 300 GPa.

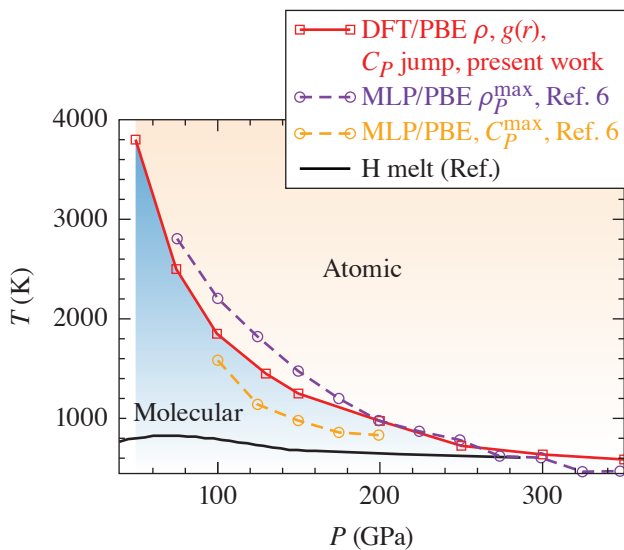


Figure 2

The LLPT boundary from the present large-scale MD-DFT (DFT/PBE) simulations compared to MLP (MLP/PBE) C_P^{max} and ρ_P^{max} curves.

TC15636JR

Given that neither the finite-size nor simulation duration diagnosis advanced in Ref. 6 is sustained by direct-calculation of chemically distinct regimes (molecular, atomic) of the hydrogen, we conclude that the MD-MLP results for the LLPT do not reproduce the fundamental MD-DFT results as they should. Up to 2048 atoms and 10-ps simulation duration, our results are consistent with the earlier subcritical behavior predictions.

V. V. Karasiev, J. Hinz, and S. X. Hu were supported by the Department of Energy National Nuclear Security Administration Award Number DE-NA0003856 and U.S. National Science Foundation PHY Grant No. 1802964. S. B. Trickey was supported by Department of Energy Grant DE-SC0002139. This research used resources of the National Energy Research Scientific Computing Center, a DOE Office of Science User Facility supported by the Office of Science of the U.S. Department of Energy under Contract No. DE-AC02-05CH11231. Part of the computations were performed on the Laboratory for Laser Energetics HPC systems.

1. E. Gregoryanz *et al.*, *Matter Radiat. Extremes* **5**, 038101 (2020).
2. J. Hinz *et al.*, *Phys. Rev. Research* **2**, 032065(R) (2020).
3. G. Rillo *et al.*, *Proc. Natl. Acad. Sci.* **116**, 9770 (2019).
4. B. Lu *et al.*, *Chin. Phys. Lett.* **36**, 103102 (2019).
5. C. Pierleoni *et al.*, *Proc. Natl. Acad. Sci.* **113**, 4953 (2016).
6. B. Cheng *et al.*, *Nature* **585**, 217 (2020).
7. J. P. Perdew, K. Burke, and M. Ernzerhof, *Phys. Rev. Lett.* **77**, 3865 (1996); **78**, 1396(E) (1997).
8. A. Baldereschi, *Phys. Rev. B* **7**, 5212 (1973).
9. G. Kresse and J. Furthmüller, *Phys. Rev. B* **54**, 11,169 (1996).
10. G. Kresse and D. Joubert, *Phys. Rev. B* **59**, 1758 (1999).
11. V. Kapil *et al.*, *Comput. Phys. Commun.* **236**, 214 (2019).
12. P. Giannozzi *et al.*, *J. Phys.: Condens. Matter* **29**, 465901 (2017).
13. W. Lorenzen, B. Holst, and R. Redmer, *Phys. Rev. B* **82**, 195107 (2010).
14. C. S. Zha *et al.*, *Phys. Rev. Lett.* **119**, 075302 (2017).
15. H. Y. Geng *et al.*, *Phys. Rev. B* **100**, 134109 (2019).